An Optimized Room-Temperature RF-Surface Resonator for In vivo Potassium-39 MRI at 9.4 T - Simulation and Measurement Study for Cryogenic Coils

Ibrahim A. Elabyad[1], Raffi Kalayciyan[1], Nagesh Shanbhag[2], Lothar Schilling[2], and L. R. Schad[1]

[1]*Computer Assisted Clinical Medicine, Medical Faculty Mannheim, Heidelberg University, Mannheim, Germany,* [2]*Division of Neurosurgical Research, Medical Faculty Mannheim, Heidelberg University, Mannheim, Germany*

INTRODUCTION: Recent MRI studies of the Tissue Sodium-23 (^{23}Na) Concentration (TSC) revealed that an irreversible increase in local TSC occurs in permanently-damaged stroke tissue [1]. Nevertheless, monitoring the intracellular ^{23}Na concentration via Multiple Quantum Coherence (MQC) filters [2] or chemical shift reagents [3] proved to be difficult up-to-date. On the other hand, since intracellular Potassium (^{39}K) concentration is ~15 times higher than in the extracellular compartment, ^{39}K-Magnetic Resonance Imaging (^{39}K-MRI) could provide direct information about pathological changes in intracellular ion concentrations after ischemic stroke. However, ^{39}K-MRI suffers from 2.1 million times lower signal-to-noise ratio (SNR) compared to ^{1}H-MRI which is caused by ~20 times lower gyromagnetic ratio, and the much faster T_2^* decay [4]. In a recent study, a triple resonant resonator setup (^{1}H, ^{23}Na, and ^{39}K) was used to acquire a first *in vivo* ^{39}K image of the rat head at 9.4 T [5]. Yet, the SNR can be significantly increased by using a single-tuned surface resonator. Furthermore cryogenic cooling could be advantageous at this low resonance frequency (18.7 MHz) and small resonator dimensions (< 30 mm in diameter) [6], [7]. In this study, a single-tuned ^{39}K surface resonator was developed and tested for the measurement of ^{39}K signal of a healthy live rat brain at room-temperature (RT). In order to estimate the benefits of cryogenic cooling at 77 K and 20 K, the optimal coil geometry, the optimal coil diameter, and temperature were determined in order to maximize the receiver SNR gain for ^{39}K-MRI at 9.4 T. The EM-simulations were validated at 293 K and 77 K for the optimal coils through bench level measurements.

MATERIALS AND METHODS: A single-loop double-tuned ^{39}K (18.7 MHz) RF-surface coil of 25-mm diameter was developed as shown in Fig. 1. A variable capacitor of 1-120 pF and three fixed capacitors of (1000 pF, 200 pF, and 160 pF) were connected in parallel to tune the coil at the resonance frequency of 18.7 MHz. The RF-coil was matched by inductive coupling to the 50 Ω signal line. The loaded/unloaded *Q*-factor ratio was measured to be 186/198. In order to geometrically decouple the developed single-loop surface coil from the ^{1}H birdcage linear resonator (Bruker BioSpin GmbH, Ettlingen, Germany), the B_1-field vector of the birdcage was orthogonally arranged to the surface coil's normal vector. No change in *Q*-factor was observed when both resonance structures were combined to form the double-resonant coil system. ^{1}H T_2-weighted images were acquired using a multi slice multi echo (MSME) sequence with TR = 1000 ms, TE = 14 ms, (0.3x0.3) mm^2 in-plane resolution with 16 axial slices of 2 mm thickness and an inter-slice distance of 2 mm. The total measurement time (TA) was 4 min and 16 sec. A 3D Chemical Shift Imaging (CSI) sequence was used for ^{39}K-MRI to achieve a voxel resolutions of 2x2x2 mm^3 (after two-fold 3D zero-filling), TR = 20 ms, and TA = 30 min. The *in vivo* experiments were carried out under appropriate animal license and ethics approval. One adult female rat (~380 g) was scanned *in vivo*. The ^{1}H edge image was superimposed onto the ^{39}K image using a routine written in MATLAB®. Full-wave Electro-Magnetic (EM)-simulations were performed using CST® Micro Wave Studio (CST AG Darmstadt, Germany) for three-coil geometries of (single-loop, spiral-two-turn, and spiral-three-turn) surface resonators with the same effective coil diameter (d_{eff}) at 293 K, 77 K, and 20 K, respectively. For all coils, 1.5-mm wire thickness was selected. The copper conductivity was set to σ_{RT}=5.7x10^7 S/m at 293 K, σ_{CT}=4.65x10^8 S/m at 77 K, and σ_{CT}=357x10^8 S/m at 20 K, respectively [8]. The S_{11}- return loss (reflection measurement on a network analyzer) was simulated and measured for all coils and the *Q*-factors were evaluated in both loaded and unloaded conditions. The sample load was modelled by a cylindrical phantom with ε_r=78, σ=0.45 S/m, 30-mm diameter, and 80-mm length. All coils were tuned and matched to the resonance frequency of ^{39}K-MRI at 9.4 T (18.7 MHz). The selected input power was 1W for all coils. To validate the accuracy of the EM-simulations for all coil geometries at 239 K and 77 K, (10-surface resonators for each type) were built in house and compared via bench level measurement methods. To measure the *Q*-factors at 293 K and 77 K, all resonators were matched by inductive coupling and tuned at 18.7 MHz and measured from the S_{11}-return loss. The unloaded *Q*-factors at 77 K were measured by immersing each coil inside an insulating polystyrene foam box filled with liquid nitrogen (LN_2). Port 1 of the network analyzer was connected with an inductive coupling loop to match the coils inside LN_2. The SNR gains for all coils were estimated using the following equations [6], [7], [9]:

$$\frac{SNR_{CT}}{SNR_{RT}} = \sqrt{\frac{R_{coil,RT}T_{coil,RT} + R_{sample}T_{sample}}{R_{coil,CT}T_{coil,CT} + R_{sample}T_{sample}}} \quad (1)$$

$$\frac{SNR_{CT}}{SNR_{RT}} = \sqrt{\frac{RT.Q^{-1}_{unloaded.RT} + RT.Q^{-1}_{sample}}{CT.Q^{-1}_{unloaded.CT} + RT.Q^{-1}_{sample}}} \quad (2)$$

$$Q^{-1}_{sample} = Q^{-1}_{loaded} - Q^{-1}_{unloaded} \quad (3)$$

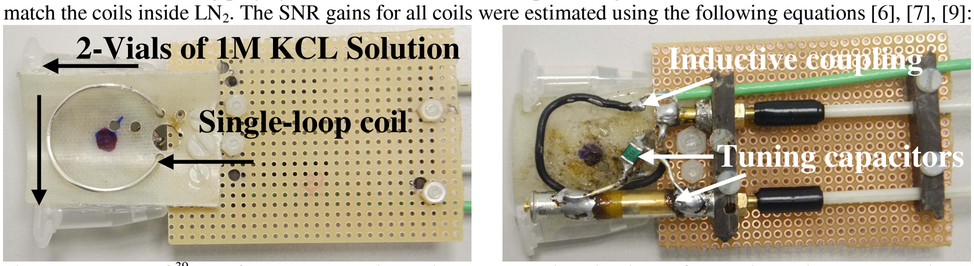

Fig. 1. Prototype of ^{39}K surface resonator with tuning and matching circuits. Left (top view), right (bottom view).

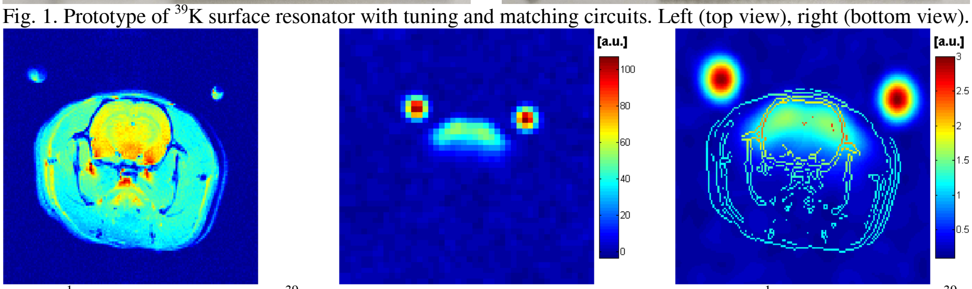

Fig. 2. ^{1}H image (first column), ^{39}K SNR-map (second column), and the superimposed ^{1}H edge image with ^{39}K image (third column).

Once the steady state of the EM-simulation at each temperature was obtained, the *Q*-factors were evaluated in both loaded and unloaded conditions. Both coil and sample resistances can be evaluated as follows: $R_{coil}=\omega L/Q_{unloaded}$ and $R_{sample}=\omega L\ [1/Q_{loaded} - 1/Q_{unloaded}]$. The sample temperature T_{sample} was assumed to be 305 K [6], [9].

RESULTS AND DISCUSSION:
The ^{1}H and ^{39}K images are shown in Fig. 2. The SNR achieved in the ^{39}K images was 35±13 in (4x4x4) mm³ voxel size and 30 min acquisition time. Previously a SNR of 4 was achieved in similar *in vivo* experiment of a healthy live rat brain using a 3D FLASH sequence, (3x3x6) mm^3 voxel size and 54 min acquisition time [5]. Hence, the herein used CSI technique in conjunction with improved resonator sensitivity achieved approximately eight times higher SNR in half the acquisition time. The simulated and measured *Q*-factors and the corresponding SNR gains for RF-coils of d_{eff} 18-mm are listed in Table I. For multi-turn spiral coils, the predicted sensitivity gain decreases compared to a single-loop coil of the same size because both R_{coil} and R_{sample} increase with increasing the coil size and the number of turns. Cryogenic cooling of the optimal single-loop cooper coil of 18-mm diameter could further improve the SNR gain three-fold at 77 K and up to six-fold at 20 K. These significant results could further improve the available signal in future ^{39}K-MR imaging studies of the rat brain at 9.4 T.

CONCLUSION: The single-loop coil is the optimal coil geometry at 293 K, 77 K, and 20 K. Cryogenic cooling of the optimal resonator can improve the SNR up to six-fold at 20 K indicating that the ^{39}K-MRI signal in cerebral tissue of the rat can be spatially resolved with (2x2x2) mm³ voxel size in 10 min acquisition time.

Coil Type d_{eff} (18-mm)	Simulated					Measured					
	293 K	77 K		20 K		293 K			77 K		
	Q_L/Q_U	Q_L/Q_U	SNR_{gain}	Q_L/Q_U	SNR_{gain}	Q_L/Q_U	R_cT_c	R_sT_s	Q_U	R_cT_c	SNR_{gain}
Single-Loop	131/133	385/422	3.22	1858/3746	7.58	147/150	7.93	0.17	319	0.96	2.68
Spiral-Two-Turn	155/168	428/525	2.54	1585/4586	3.54	185/193	16.93	0.75	464	1.82	2.62
Spiral-Three-Turn	168/186	455/591	2.41	1443/5236	3.18	257/272	28.75	1.72	668	3.01	2.54

REFERENCES: [1] Wetterling *et al*., MRM 67, 740–749 (2012). [2] Tyson *et al*., Stroke 27, 957–964 (1996). [3] Heiler *et al*., JMR 34, 935–940 (2011). [4] Parrish *et al*., MRM 38, 653–661 (1997). [5] Augath *et al*., JMR 200, 134–136 (2009). [6] Darrasse *et al*., BIOCHIMIE 85, 915–937 (2003). [7] Wright *et al*., MRM 43, 163–169 (2000). [8] Thompson *et al*., Cryogenic properties of copper. NIST, Boulder, Colorado (1990). [9] Hu *et al*., IEEE I&M 61, 129–139 (2012).